

Fabrication and *in vitro* evaluation of polyvinyl alcohol/bio-glass composite for potential wound healing applications

T. Khan^{a,b,*}, E. H. Mirza^a, N. J. Kurd^a, M. Naushad^{a,c}, M. Z. Ul Haque^b

^a*Department of Biomedical Engineering, NED University of Engineering and Technology, Karachi, Pakistan*

^b*Department of Biomedical Engineering, Salim Habib University, Karachi, Pakistan*

^c*Department of Biomedical Engineering, Faculty of Engineering Science Technology and Management, Ziauddin University*

In this study, a novel composite is fabricated by incorporating Polyvinyl alcohol (PVA) and Bio-Glass (BG) *via* the freeze-thaw method. PVA pre-polymer is prepared in three different concentrations i.e. (2%, 5%, and 10%) by dissolving PVA powder in distilled water by using a hot plate magnetic stirrer at 80° C, and a constant concentration of BG i.e 2% is added into each PVA prepolymer. Total six specimens including (PVA (2%), PVA (5%), PVA (10%), PVA (2%)/BG (2%), PVA (5%)/BG (2%), and PVA (10%)/ BG (2%) were prepared in which pure PVA specimens acts as a control group. The physicochemical and mechanical properties of the specimens were examined. Various characterization tests such as scanning electron microscopy (SEM), swelling analysis, degradability analysis, hygroscopicity, pH sensitivity, tensile analysis, gel fraction test, water vapor transmission rate (WVTR), and contact angle analysis were performed on the samples. SEM analysis showed that with the increase in PVA concentration, the material becomes smoother and more compact. Results from the current study showed that tensile strength, degradation rate, and gel content are directly proportional to PVA concentration, while swelling capacity, pH sensitivity, hygroscopicity, WVTR, and hydrophilicity are inversely related to PVA concentration. Moreover, with the addition of BG, tensile strength, degradation rate, pH sensitivity, swelling capability, hydrophilicity, and, gel content of the specimens is increased, whereas, WVTR is decreased and, hygroscopicity remains unchanged. Furthermore, results from this study must be taken a step ahead & biocompatibility must be tested to evaluate the biological performance.

(Received April 7, 2023; Accepted July 12, 2023)

Keywords: Bio-glass, Bioactive, Bio-degradable, Freeze-thaw, Hydrogel, Polyvinyl alcohol, Wound healing

1. Introduction

The human skin is the most extensive and vital tissue of our human body as it acts as a protective layer between internal organs and the surrounding environment [1,2]. Against external barriers, skin acts as the first line of defense [3]. Wounds are the result of an interruption to skin integrity due to any physical trauma, injury, or disease [4]. Acute wounds occur as a consequence of any sudden injury, accident, or trauma and heal promptly, whereas, chronic wounds cannot be able to cure promptly [5]. Complex and chronic wounds are mostly hard to heal which results in anxiety, discomfort, and reduced quality of life for patients and they also need a huge amount to treat [6,7]. Wound healing is an intricate process involving coordinated interactions [8]. It includes a cascade of carefully and accurately controlled steps and events correlative to the appearance of different cell types during different phases of the healing activity in the wound bed [7,9]. Wound dressings are usually used to fasten up the healing process. According to wound type, an appropriate dressing must be selected. An ideal wound dressing should be innocuous, non-adhesive, provide a

* Corresponding author: tooba.khan@shu.edu.pk
<https://doi.org/10.15251/DJNB.2023.183.821>

damp environment, permit gas interchange, promote epidermal migration, angiogenesis, and connective tissue synthesis, and inhibit bacteria and pathogens from entering the body [10-13]. From previous studies, it is obvious that wound healing is the subject of focus for decades [9,10]. Films, Gauze, Hydrocolloids, Hydrogels, Foams, and Alginates are most commonly found in previous studies with some limitations. Gauzes are inexpensive but cause injury when removed, films contain moisture hence can only be utilized for non-exudative wounds, Hydrocolloids enhance fluid trapping hence cannot be used for infected wounds, Hydrogels, and Alginates can't be used for dry wounds, and similarly, tissue-engineered skin substitutes are quite expensive [11,12,14,15] Due to the rising elderly population with chronic wound history, demands for wound healing products are also increasing [4]. Developed countries spent almost 2-3% of their total healthcare budget on the cure of chronic wounds [6]. To minimize the burden on healthcare expenditures and to minimize patient pain and anxiety, there is an utter need to develop new and advanced wound care technologies.

A new alternative is the use of Bio-Glass (BG) as a wound healer. BG is a well-known bioactive and biodegradable material that has been utilized for hard tissue regeneration. It is a rigid, non-permeable, and hard material, which is categorized as Bio-Ceramics. It is the first identified artificial material and has outstanding bone-binding capabilities [16]. Bioactive Glass or Bio-glasses are composed of $\text{SiO}_2\text{-CaO-Na}_2\text{O-P}_2\text{O}_5$ [17]. Different sorts of BG can be fabricated by tailoring the percentage of the components [18]. It has been investigated that BG or bioactive glasses have shown excellent capabilities in regenerating bone. The use of BG is not limited only to hard tissue applications but can also be utilized for soft tissue regeneration. Due to its ability to promote angiogenesis and osteogenesis, it has gained a lot of attention in the field of Tissue Engineering [17].

Wound healing consists of four processes including Hemostasis Phase, Inflammatory Phase, Cell Proliferation Phase, and ECM remodeling Phase [18,19]. Several studies have been conducted in recent years to investigate the role of bio-glass in each phase of wound healing and all these studies indicate that bio-glass have shown promising results in each phase of wound repair by accelerating the cellular interaction of endothelial cells, inflammatory cells, and fibroblasts [20,21]. Some researchers have also analyzed that the ionic by-products released when BG interacts with human body fluids fasten up the wound healing process [22,23]. This glass shows excellent bioactivity and it can vary from surface bioactive to bulk degradable which means it can be resorbed in 10-30 days in the tissue [24]. Bio-glass promotes rapid ion exchanges in contact with body fluids, which creates an alkaline environment on the surface that enhances imine bond formation and thus increases the hydrogel adhesiveness to tissues [12].

Polyvinyl alcohol (PVA) is a water-soluble polymer that is usually created through hydrolysis using polyvinyl acetate [25]. Water absorption of PVA is decreased by crosslinking the PVA chains [26]. PVA is ductile but strong, and flexible. PVA has several properties, which makes it extremely useful for medical applications [27]. It is biocompatible, has the excellent film-forming ability, and is also non-carcinogenic, and hydrophilic with low frictional function [28]. PVA also exhibits high tensile strength and excellent adhesiveness [29]. Not only this, but PVA hydrogels also have a high degree of swelling in water/biological fluids, and are very much capable of simulating natural tissues. PVA hydrogels also exhibit excellent elasticity [30], which is considered to be an important parameter when considering biomaterials for tissue engineering applications [31]. Moreover, studies show that PVA-based composites can be configured for enhancing different mechanical properties [32]. The PVA was discovered to be quite helpful as an injury-healing accelerator [33]. Current research focuses on the fabrication of a biomaterial incorporating BG and polyvinyl alcohol (PVA). The objective of this study is to fabricate a Bio-Glass/PVA composite having skin-mimicking properties. Further, the physicochemical and mechanical characteristics of the fabricated composite have been examined in this study. The fabricated material will certainly accelerate the wound-healing process. This study will also help in reducing time and expenditure for the wound healing process. Furthermore, it will be beneficial for using BG with naturally occurring Bio-Materials as compared to synthetic ones for skin regeneration purposes.

2. Materials and methods

2.1. Materials

PVA powder having molecular weight 89,000-98,000 g/mol and reagent grade pure Bio-Glass (45S5, $\geq 98\%$, 0.2-500 μm particle size) powder were procured from Sigma Aldrich. Other materials include Hydrochloric Acid (HCl), Sodium Chloride (NaCl), Tris (hydroxymethyl) aminomethane ((CH_2OH)₃CNH₂), Sodium Bicarbonate (NaHCO₃), Sodium Sulphate (Na₂SO₄), Potassium Hydrogen Phosphate Trihydrate (K₂HPO₄·3H₂O), Potassium Chloride (KCl), Magnesium Chloride Hexahydrate (MgCl₂·6H₂O) and Calcium Chloride (CaCl₂), were also procured from Sigma Aldrich.

2.2. Preparation of simulated body fluid (SBF) solution

Simulated Body Fluid (SBF) has a similar inorganic ion composition as human body fluid [34,35]. The technique mentioned in the previous study was adopted for the preparation of SBF solution with minor modifications [36]. Firstly, 750 ml of de-ionized water is filled in a polyethylene beaker, followed by dissolving NaCl (7.996 g), NaHCO₃ (0.350 g), KCl (0.224 g), K₂HPO₄·3H₂O (0.228 g), MgCl₂·6H₂O (0.305 g), CaCl₂ (0.278 g), and, Na₂SO₄ (0.071 g) one by one with vigorous stirring at 36.5 °C. After adding all reagents, the pH of the solution was adjusted to 7.40 with the addition of (CH_2OH)₃CNH₂ (6.057 g) for increasing the pH value and 1M HCl solution for dropping the pH value to 7.40. After adjusting the pH of the prepared SBF solution to 7.40 at 36.5 °C, the beaker was filled with de-ionized water up to the marked line of 1000 ml. This freshly prepared SBF solution is preserved in a plastic bottle at 5 – 10 °C and was used within 30 days.

2.2. Synthesis of pre-polymer and preparation of PVA & PVA/BG specimens

The PVA and PVA/BG specimens were fabricated using the freeze-thaw method as described in our previous study with a brief modification [37]. The composite was prepared in varying w/w percentages of PVA i.e., 2% (w/v), 5% (w/v), and 10% (w/v), these w/w percentages were selected as soft materials are required for wound healing applications and literature suggests that with the increase in PVA concentration, the crosslinking is also increased due to which elasticity is greatly reduced [38]. The constant concentration of BG was utilized in this study i.e., 2%, as the wound healing process is more enhanced at minimal concentrations of Bio-Glass due to enhanced macrophage proliferation [39]. Preparation of pure PVA specimens involves the preparation of PVA solution at 80°C with the aid of magnetic stirring. To prepare 2% (w/v), 5% (w/v), and 10% (w/v) PVA solution, 2 grams, 5 grams, and 10 grams of PVA powder underwent dissolution in 98 mL, 95 mL, and 90 mL of distilled water respectively. The mixture was then subjected to hydrolysis using a hot plate magnetic stirrer at a temperature of 80°C for 1.5 hours. PVA/BG solution was prepared by dissolving 0.2 grams of Bio-glass to each 2% (w/v), 5% (w/v), and 10% (w/v) of pure PVA solution and then sonicated for 1 hour at 50% power. The preparation of pure PVA and PVA/BG specimens with the freeze-thaw method is represented in Figure 1(a) and 1(b) respectively.

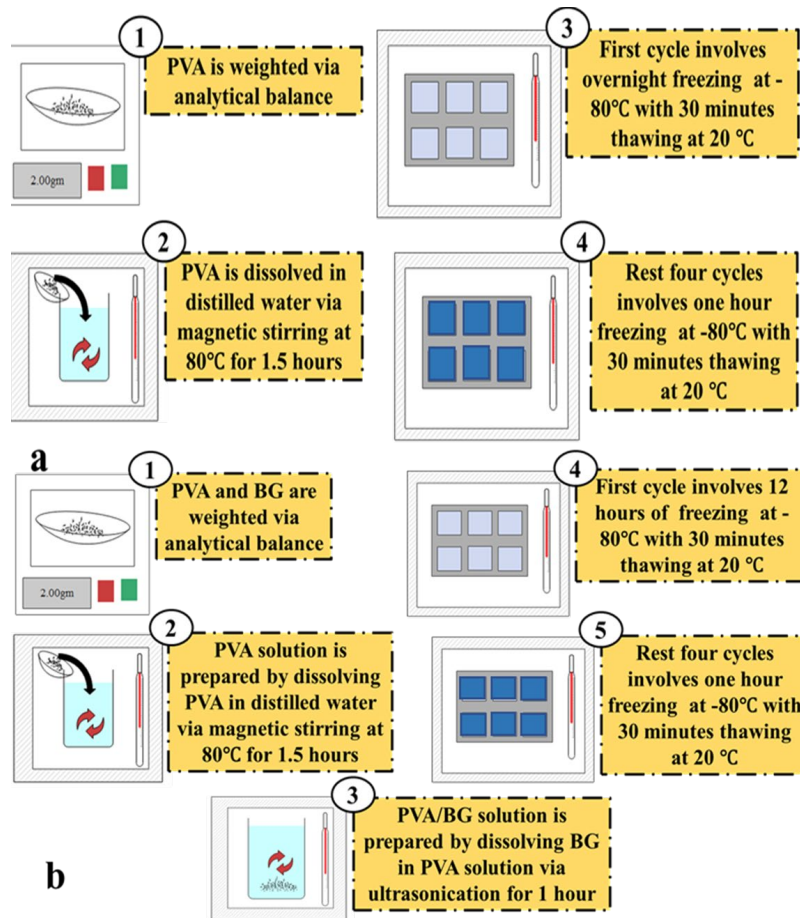


Fig. 1. Synthesis of Pure PVA and PVA/BG specimens by Freeze-Thaw Method.

Once the pure PVA and PVA/BG pre-polymer were ready, then, 5 mL of each pre-polymer was poured into silicone molds to get pure PVA and PVA/BG specimens. The pre-polymer was then placed in BIOBASE BDF-86V158 ultra-low temperature freezer for 5 cycles. The specimens were kept at -80°C for 12 hours followed by 30 minutes of thawing at 20 °C for the 1st cycle whereas, for the rest of the four cycles, specimens were kept at -80°C for 1 hour with 30 minutes of defrosting at 20 °C.

2.3. Characterization and analysis

The fabricated specimens were tested and analyzed by performing various characterization tests such as Scanning Electron Microscopy, Tensile, pH sensitivity, Swelling, Degradation, Moisture content, gel fraction, water vapor transmission rate, and contact angle analysis.

2.3.1. Scanning Electron Microscopy

Scanning electron microscopy (SEM) test was performed at “The Centralized Science Laboratory”, Karachi University, located in Pakistan to observe the topographical image of the fabricated specimens. All specimens were cut into 1 cm² piece, coated with gold as a conductive material, and then placed into JEOL Scanning Electron Microscope having model JSM-6380A. The operating voltage of the microscope is 20kV. PVA and PVA/BG specimens were analyzed using SEM and images were captured at a magnification level of 1000 and 2300.

2.3.2. Swelling analysis

The swelling test was performed by immersing the specimens in simulated body fluid (SBF), by the protocol mentioned in the study [40]. Each specimen of 1 cm² was submerged in 4ml of SBF, having a pH of 7.4 at room temperature for 5 hours in sterile Petri dishes. All the specimens were

weighed initially using analytical balance KERN ABS80-4N before immersing them in solution and reweighed up to 4 hours every hour and further for 2 weeks. For weight measurement, the specimens were removed from the medium and excessive SBF solution is removed with the help of filter paper. The medium was replaced weekly. Swelling percentages were calculated using Eq. 1:

$$\text{Swelling (\%)} = \left[\frac{(W_s - W_o)}{W_o} \right] \quad (1)$$

where ‘ W_s ’ is the swelled weight of specimens at different time intervals and ‘ W_o ’ is the initial dry weight of the specimens.

2.3.3. Degradation test

The degradation of the specimens was evaluated through immersion in a simulated body fluid (SBF) solution. Each specimen of 1 cm² was submerged in 4ml of SBF solution, having pH 7.4 at room temperature for 5 weeks in disinfected Petri dishes. All the specimens were weighed initially using analytical balance KERN ABS80-4N before immersing them in solution and reweighed up to 4 hours for every hour and further for 5 weeks every week. For weight measurement, the specimens were removed from the medium and excessive SBF solution is removed with the help of filter paper. The medium was replaced weekly and degradation percentages were calculated using Eq. 2

$$\text{Degradation (\%)} = \left[\frac{(W_t - W_o)}{W_o} \right] \quad (2)$$

where ‘ W_t ’ is the weight of specimens at different time intervals and ‘ W_o ’ is the initial weight of the specimens.

2.3.4. Moisture content

Moisture content test was performed by placing the pre-weighted specimens in a drying oven at 60 °C for 24 hours. The specimens were re-weighted after 24 hours to determine the moisture present in the specimens. The moisture content was calculated by using Eq. 3

$$\text{Moisture content (\%)} = \left[\frac{(M_{\text{moist}} - M_{\text{dry}})}{M_{\text{dry}}} \right] \quad (3)$$

where ‘ M_{moist} ’ is the weight of the moist specimens and ‘ M_{dry} ’ is the weight of the dry specimens.

2.3.5. pH sensitivity

The pH sensitivity of the specimens was analyzed by immersing the pre-weighted specimens in 4ml PBS solution having pH 2.25, 4.6, 6.16, and 7.4. The specimens were evaluated every 15 minutes for 1 hour then after 2 hours and last they were evaluated at 1 week. The specimens were removed from the medium and excessive PBS solution was removed with filter paper. The pH sensitivity was determined by using Eq. 4

$$\text{Weight change (\%)} = \left[\frac{(W_t - W_o)}{W_o} \right] \quad (4)$$

where ‘ W_t ’ is the weight of specimens at different time intervals and ‘ W_o ’ is the initial weight of the specimens.

2.3.6. Tensile strength

To determine the strength and elasticity of fabricated specimens, a tensile test was performed following the ASTM standard D3039 [41], using an electronic universal testing machine (UTM) of model WDW-2M. The prepared specimens were cut into a rectangular shape of 250 mm in length, and 25 mm wide with a thickness of 1 mm.

2.3.7. Contact angle

Contact Angle test was performed to analyze the wettability properties of the samples. The prepared samples were air-dried naturally at room temperature and the water contact angles of the samples were measured using a dynamic contact angle measurement instrument with model number HO-IAD-CAM-01, employing the sessile drop method, using the protocol mentioned in the study [42].

2.3.8. Gel fraction

The specimens were cut into 10 x 10 mm pieces to perform the gel fraction test. The specimens were placed in a drying oven at 40 °C for 24 hours and then weighed (W_o). The dried specimens were then placed into deionized water for 48 hours until they reached a swelling equilibrium. The specimen was then dried at 40°C for 24 hours and then reweighed (W_e) to determine the gel fraction. The gel fraction in the specimens was calculated using equation 5.

$$\text{Gel Content}(\%) = \left[\frac{W_e}{W_o} \right] \times 100 \quad (5)$$

where ' W_e ' is the final weight of specimens and ' W_o ' is the initial weight of the specimens after drying.

2.3.9. Water vapor transmission rate

The water vapor transmission rate (WVTR) test was calculated by the protocol described in this study [43]. The test was conducted by taking 10mL deionized water in a glass bottle having diameter 35mm. The specimens were placed on the mouth of the glass bottle and tightened using Teflon tape. The glass bottle along with the specimen cap was weighed initially (W_i) and then placed in a drying oven at 40°C for 24 hours and then reweighed (W_f). The water vapor transmission rate was calculated using equation 6.

$$\text{WVTR} \left(\frac{\text{g}}{\text{m}^2 \cdot \text{T}} \right) = \left[\frac{W_i - W_f}{A} \right] \times T \quad (6)$$

where ' W_f ' is the final weight of glass bottle, ' W_i ' is the initial weight of the glass bottle, ' A ' is the area of the mouth of the glass bottle in m^2 , and ' T ' is the duration of incubation i.e 24 hours.

2.3.10. Statistical analysis

The Univariate Analysis of Variance was performed to assess the differences between sets of data. The statistical analysis was conducted using Microsoft Excel, and a significance level of $p < 0.05$ was established.

3. Results and discussion

3.1. Scanning Electron Microscopy

The surface morphology of pure PVA and PVA/BG specimens was studied to investigate the changes in surface properties that occur with the increase in PVA concentration and after the addition of BG.

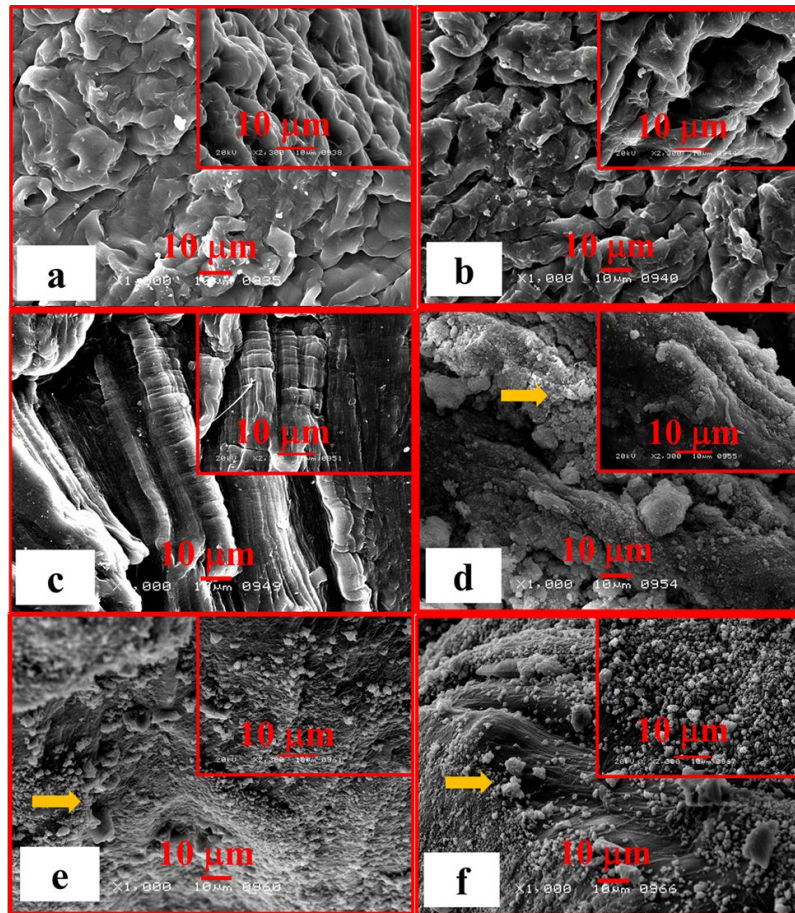


Fig. 2. SEM results of (a) Pure PVA 2% (b) Pure PVA 5% (c) Pure PVA 10% (d) PVA 2% /BG 2% (e) PVA 5% /BG 2% (f) PVA 10% /BG 2%, Yellow arrows represents BG deposition on the surface.

Figure 2 represents the SEM results of Pure PVA and PVA/BG specimens. The incorporation of bio-glass is evident by SEM analysis in all concentrations and is represented by yellow arrows. In figure 2 (a), we can observe that the specimen structure is rough due to the lower concentration of PVA, whereas, in figure 2 (b-c) we can observe a smooth and more compact structure due to a higher concentration of PVA. Figure 2 (d-f) represents the SEM images of PVA/BG specimens in which the incremental composition of BG particles is visible.

The results indicate that Pure PVA 2% and 5% specimens represent a honeycombed structure containing a gap in between the polymer chains whereas 10% pure PVA specimens are more crosslinked and compact. The BG particles are visible on the surface of the specimens. In 2% and 5%, PVA/BG specimens the BG particles are submerged in between the polymer chains whereas in 10% PVA/BG specimens the BG particles are visible on the surface of the specimens. The results obtained are quite similar to those mentioned in the previous study [44].

3.2. Swelling analysis

Swelling analysis was carried out to evaluate the fluid uptake capabilities of the specimens, which is considered to be a profound factor in wound healing [45]. The swelling rates of PVA and PVA/BG specimens at different time intervals are represented in Figure 3. It is evident that maximum swelling capability is observed by 2% pure PVA specimens which is around $52\% \pm 3\%$ after 2 weeks. A significant difference ($p < 0.05$) is observed in specimens with the increase in PVA concentration and also there is a significant difference with the addition of BG in 2% concentration specimens at the end of 3 weeks. Pure PVA specimens indicate a slight increase in their swelling ratios than the PVA/BG 2% and 5% specimens, whereas 10% specimens depict similar swelling capabilities at different time intervals. There is a noteworthy difference in the

swelling capabilities of 2%, 5%, and 10% specimens. It was also observed that the swelling ratio depends on the concentration of PVA. The swelling results represent that the swelling decreases as the concentration is increased, this is because swelling mainly depends on the composition of the hydrogel. As the concentration of polymer increases, the number of ordered polymer chains also increases. This is the reason why decreased swelling ratios were observed with increasing concentration [46]. It can also be observed that the swelling ratio is decreased with the addition of BG, this is because BG particles act as an additional cross-linker [47]. Biomaterials having hydrophilic polymer are more receptive to water and moisture present in the surrounding environment. These materials exhibit hygroscopic properties due to the existence of hydrophilic groups in their macromolecule chains. Swelling is a major factor in the evaluation of materials used in drug release, wound healing, and various other applications [48].

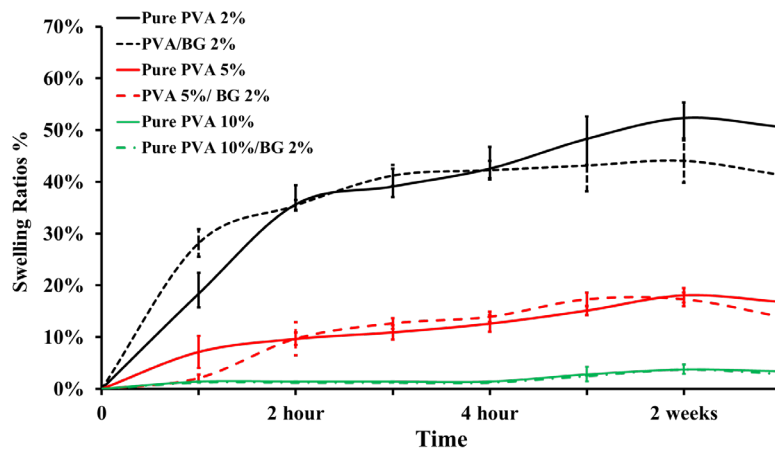


Fig. 3. Swelling ratios of Pure PVA & PVA/BG hydrogel specimens immersed in SBF for 3 weeks.

3.3. Degradation test

Degradation test was carried out to evaluate the degradation capabilities of samples over a special period of time. The percentage weight change of PVA and PVA/BG specimens at different time intervals is represented in Figure 4. Results indicate that a significant difference ($p < 0.05$) is observed with the addition of BG in 2% concentration at 3 weeks and also a significant difference is observed between the degradation rate of 2%, 5%, and 10% concentrations. It is evident from the results that the degradation is observed after 2 weeks and maximum degradation is observed in 10% of specimens. 2% and 5% PVA/BG specimens depict less degradation than pure 2% and 5% specimens, whereas, in 10% concentration, both pure PVA and PVA/BG specimens represent a similar degradation profile.

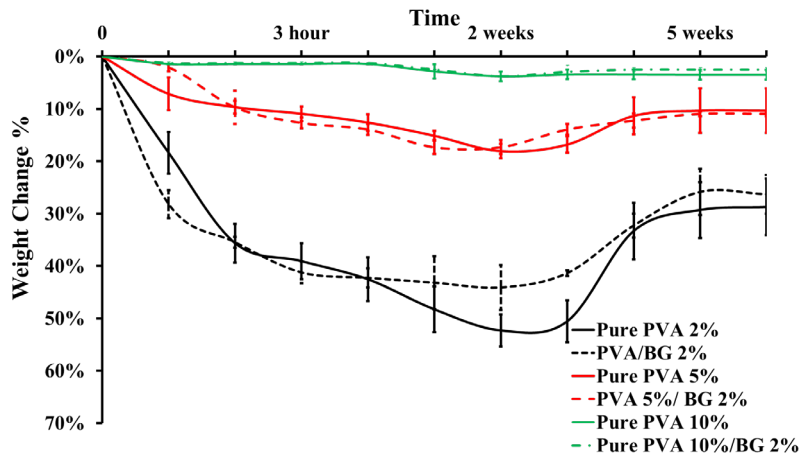


Fig. 4. Degradation Percentages of Pure PVA & PVA/BG hydrogel specimens immersed in SBF for 6 weeks.

Overall degradation percentages at the end of week 6 are represented in figure 5. We can observe that the degradation rate was decreased as the concentration of PVA was increased, this is because, with the increase in PVA concentration, the microcrystalline area, and the junction joints are increased which in turn enhances the water-retaining capacity of the specimens. Higher the PVA concentration, the higher the water-retaining capacity, and the slower the water-loss ability [49]. It can also be observed from the graph that with the addition of BG the degradation rate is slightly decreased, that is because BG particles act as an additional crosslinker in between the PVA polymer chain. Degradation is considered one of the prime features of biomaterials required for wound healing applications. The degradation rate is an important parameter that indirectly regulates the functionality of cells and the remodeling of the host tissue [47].

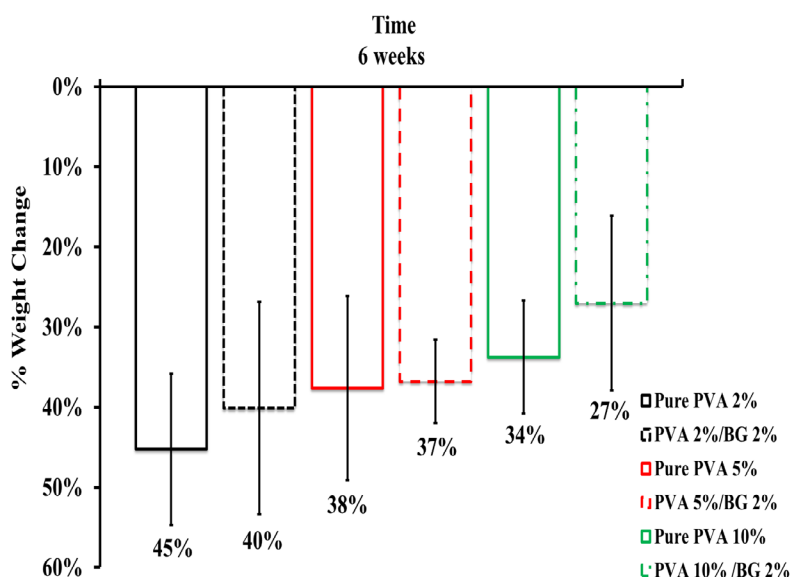


Fig. 5. Degradation Percentages of Pure PVA & PVA/BG hydrogel specimens at week 6.

It is evident from the results that maximum degradation at the end of week 6 is observed by 2% (w/v) Pure PVA specimens i.e. $45\% \pm 9.43\%$ whereas the least degradation rate was observed by PVA (10%)/BG (2%) specimens i.e. $27\% \pm 10.92\%$.

3.4. Moisture content

Moisture content was analyzed to determine the hygroscopic behavior of the fabricated specimens. The specimens showed a significant reduction in their size before and after placing them in the drying oven as represented in Figure 6.

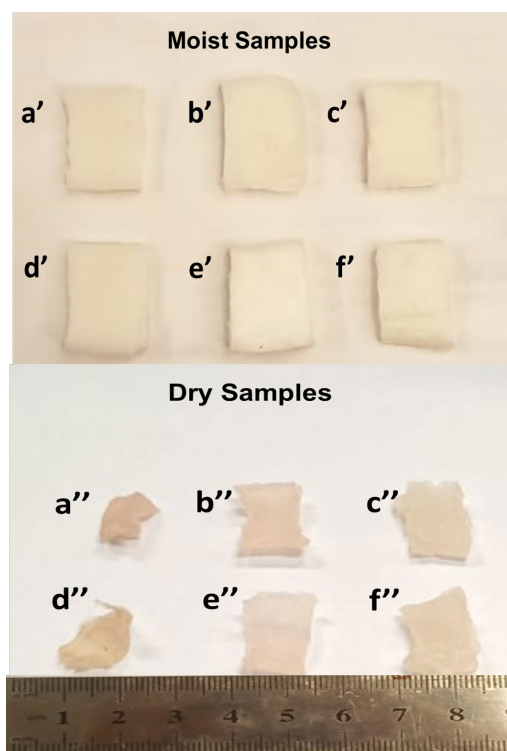


Fig. 6. Moist specimens of (a') Pure PVA 2% (b') Pure PVA 5% (c') Pure PVA 10% (d') PVA 2%/BG 2% (e') PVA 5%/BG 2% (f') PVA 10%/BG 2% and Dry specimens of (a'') Pure PVA 2% (b'') Pure PVA 5% (c'') Pure PVA 10% (d'') PVA 2%/BG 2% (e'') PVA 5%/BG 2% (f'') PVA 10%/BG 2% .

The change in moisture content and the hygroscopic behavior of hydrogels [50], in all specimens over the period of 24 hours can be analyzed in figure 7. Results indicate that no significant difference ($p > 0.05$) is observed on hygroscopicity of specimens with the addition of BG, whereas when PVA concentration was increased from 2% to 10% a noteworthy difference ($p < 0.05$) is observed. Results indicate that maximum hygroscopicity is observed by 2% (w/v) Pure PVA/ BG specimens that is $94.69\% \pm 0.84\%$ and the least hygroscopicity is observed by 10% (w/v) Pure PVA specimens which is $90.21\% \pm 0.45\%$. Bio-Glass specimens seem to be more hygroscopic than pure specimens. 2% (w/v) pure PVA and PVA/BG specimens represent more hygroscopicity, in comparison to 5% (w/v) and 10% (w/v) specimens Results depict that with the increase in concentration, there is a decrease in the hygroscopicity of the specimens.

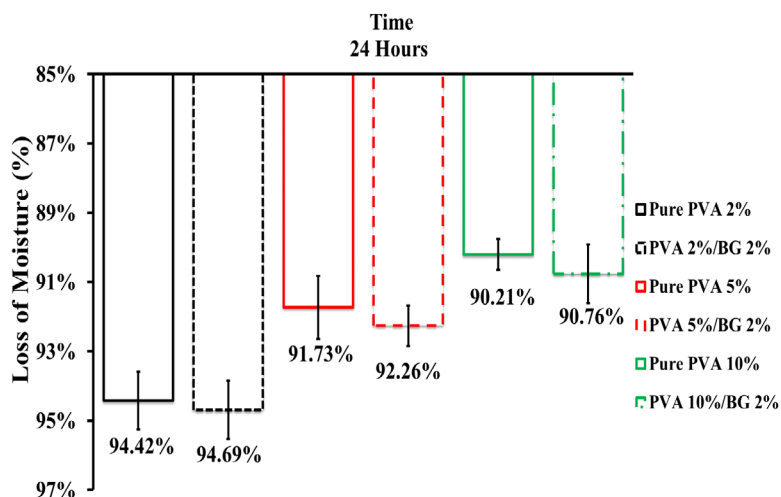


Fig. 7. Change in moisture content of Pure PVA 2%, PVA 2%/BG 2%, Pure PVA 5%, PVA 5%/BG 2%, Pure PVA 10%, and PVA 10%/BG 2% over 24 hours.

It is obvious from the results that hygroscopicity is decreased with the increase in PVA concentration this can be attributed as there is an increase in cross-linking density with the increase in PVA concentration and the microstructure becomes more closely packed and restricts the volume expansion in the hydrogel [51].

3.5. pH sensitivity

Research has shown that the water absorption capacity of hydrogels is impacted by changes in the surrounding pH. This suggests that ionic hydrogels can display swelling behavior at different pH levels [52]. Therefore, to analyze the swelling ratios of the specimens at different pH levels, a pH sensitivity test was performed.

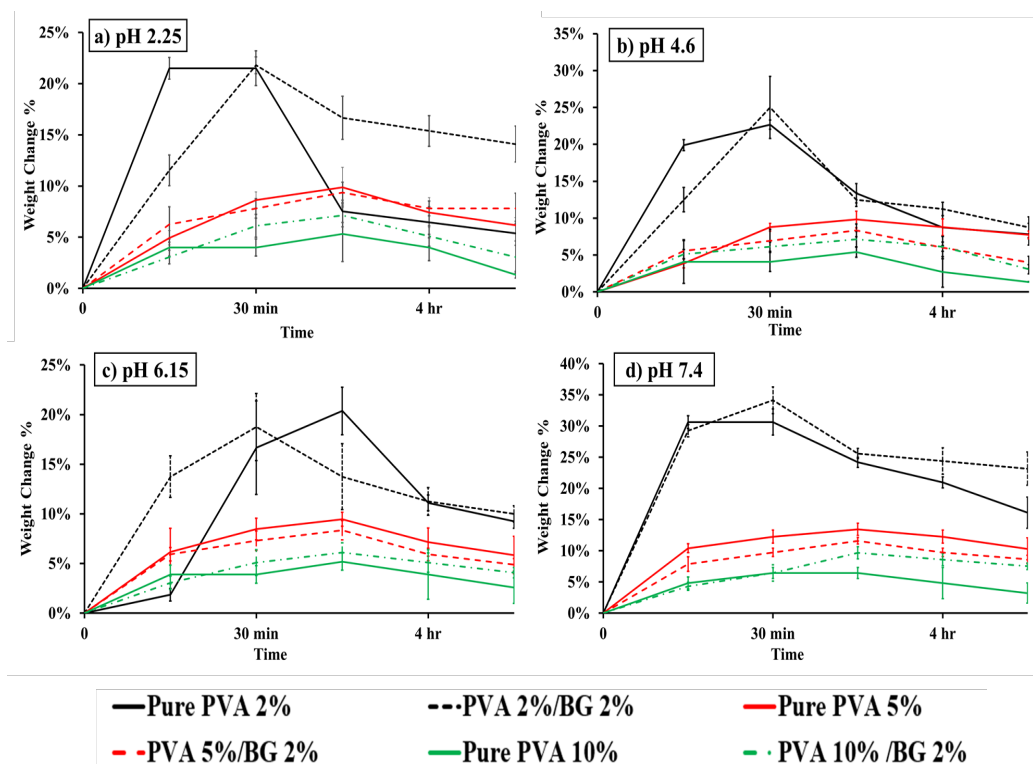


Fig. 8. Swelling ratios at (a) pH 2.25, (b) pH 4.6, (c) pH 6.15 & (d) pH 7.4 of Pure PVA 2%, Pure PVA 5%, Pure PVA 10%, PVA 2%/BG 2%, PVA 5%/BG 2%, PVA 10%/BG 2% over 4 hours.

The specimens were placed into pH 2.25, 4.6, 6.15, and 7.4 and their swelling ratios is observed. The swelling ratios of specimens at different pH values are represented in figure 8. Obtained results are quite similar to as mentioned in the previous study [53]. Results obtained indicate that initially there is swelling in the specimens followed by degradation and then after 1 week a plateau phase is observed. In all concentrations, we can observe that PVA/BG specimens have a slower degradation rate than pure specimens. Results indicate that with the increase in PVA concentrations and with the addition of BG in specimens of 2% concentration at pH 2.25, 4.6, 6.15, and 7.4 a significant difference ($p < 0.05$) is observed at different time intervals. All the specimens showed stable behavior in different pH environments. Results indicate that maximum swelling was indicated by 2% (w/v) PVA/BG specimens which is $34\% \pm 2\%$ in the 7.4 pH solution. It is noticeable from the results that pure PVA specimens degrade faster than PVA/BG specimens at all pH values. The specimens with 2% concentration of PVA represent faster degradation whereas samples with 5% and 10% concentrations of PVA indicate slower degradation behavior.

Intracellular and extracellular pH is a prime factor that affects the wound healing process. Most of the cellular processes depend on pH [50]. The skin's pH is slightly acidic and falls within the range of 4 to 6.6. However, when the skin is injured, it is exposed to internal body fluids that have a physiological pH of 7.4, leading to an increase in the pH of the affected skin [54]. It is evident from the results that the specimens were stable in all pH values and represent the highest swelling at pH 7.4, which is the pH of human blood and body fluids. Chronic wounds usually have a pH between 7.15 - 8.9 [50] and hence the fabricated specimens can be utilized for chronic wounds. It is also noticeable from the results that the fabricated specimens exhibit significant swelling ability in response to variations in the surrounding pH values. Results indicate that at pH 2.25 and 7.4, PVA (2%) / BG (2%) specimens showed higher swelling than pure PVA specimens indicating the capability of BG to interact at both acidic and neutral pH values.

3.6. Tensile analysis

Tensile results indicate that with the incorporation of bio-glass and with the elevated concentration of PVA, the tensile strength was significantly improved. The maximum stress that a 2% pure PVA specimen can bear is around 26 KPa whereas PVA/BG specimens of 2% concentration can withstand the maximum stress of around 80 KPa, as represented in Table 1. Results also indicate that the maximum stress pure PVA specimens of 5% concentration can bear is around 53 KPa whereas PVA/BG specimens of 5% concentration can withstand the stress of around 80 KPa. Pure PVA and PVA/BG specimens of 10% concentration have a similar tensile strength of 120KPa. It can also be observed that with the addition of BG, the tensile strength was increased from 26KPa to 80KPa in 2% specimens whereas, in 5% specimens, the tensile strength was increased from 53KPa to 80KPa and for 10% specimens, there is a slight increase in tensile strength from 112 KPa to 120KPa. Figure 9 represents the tensile curves from the fabricated specimens.

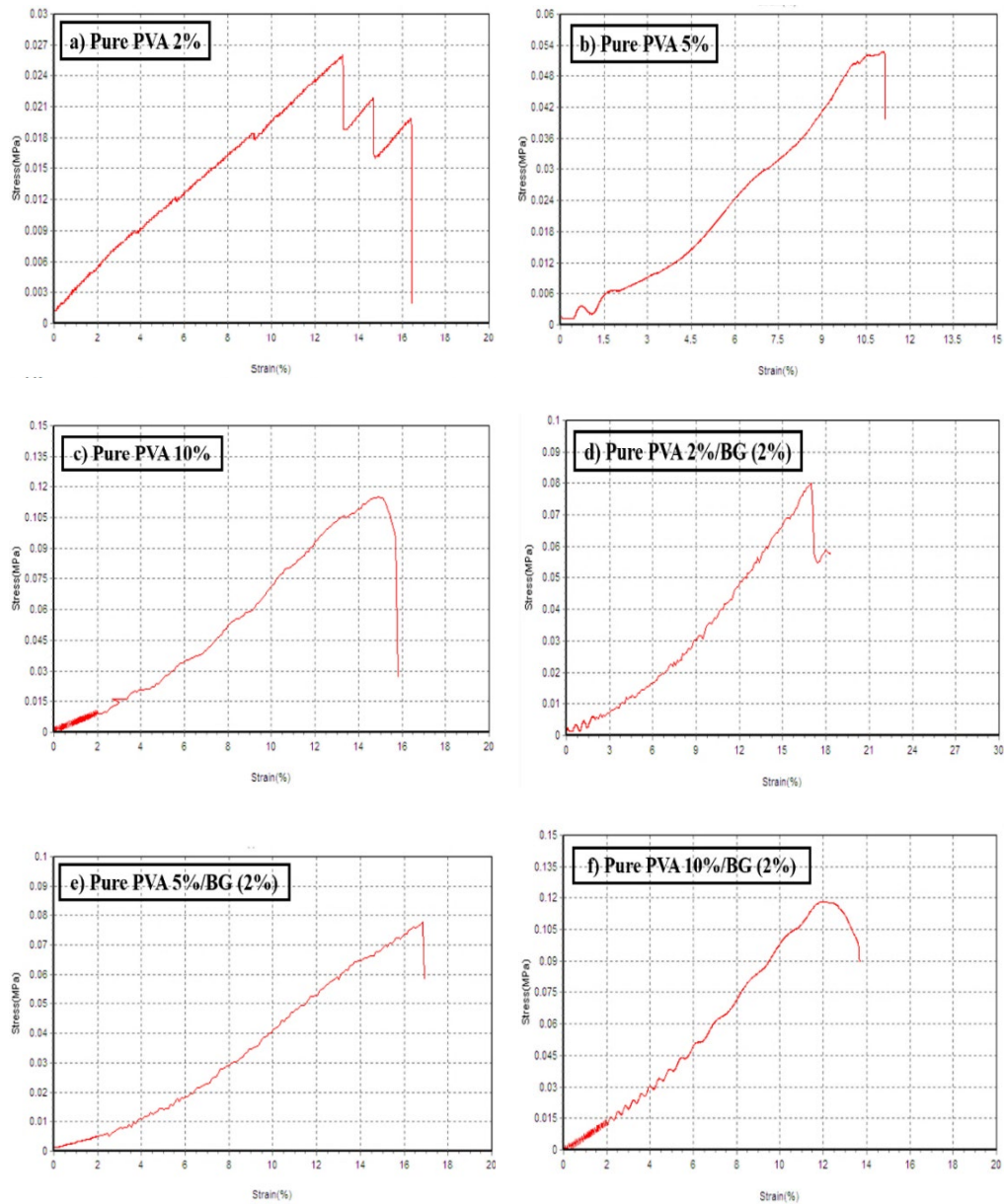


Fig. 9. Tensile results of (a) Pure PVA 2% (b) Pure PVA 5% (c) Pure PVA 10% (d) PVA 2%/BG 2% (e) PVA 5%/BG 2% (f) PVA 10%/BG 2%.

Table 1. Tensile Strength and Strains of PVA and PVA/BG Specimens.

Specimen	Tensile Strength (KPa)	Strain (%)
PVA (2%)	26	13
PVA (5%)	53	11
PVA (10%)	112	15
PVA (2%) BG (2%)	80	16
PVA (5%) BG (2%)	80	16.5
PVA (10%) BG (2%)	120	12

Results indicate that the tensile strength was increased with the increase in PVA concentration, this may be attributed as with the increase in PVA concentration, crosslinking increases which results in higher tensile strength[46]. The results obtained are quite similar as mentioned in the previous study [55]. It can also be observed from the results that with the addition of BG particles there is an increase in the mechanical properties of the PVA specimens which are quite similar to the results obtained in the previous study [44]. Results also indicate that there is no significant increase in tensile strength of Pure PVA and PVA/BG specimens of 10% concentration this is since with the increase in PVA concentration the PVA solutions become more viscous and it is difficult for BG particles to disperse in the hydrogel which results in less mechanical strength of the specimens [44].

3.7. Contact angle

Contact angle test was performed to analyze the wettability of the prepared specimens. Typically, an ideal wound dressing is hydrophilic or has a contact angle of less than 90° . Hydrophilic dressings exhibit excellent capabilities in absorbing exudates from the wound bed[56]. Results indicate that the hydrophilicity of the specimens represents no significant difference ($p > 0.05$) with the addition of Bio-Glass whereas with the increase in PVA concentration a significant difference ($p < 0.05$) is observed in between specimens. It can be observed from the results that the hydrophilicity is decreased with the increase in PVA concentration and hydrophilicity is increased with the addition of BG. This is since with the increase in PVA concentration, the crosslinking increases due to which the water absorbing capacity is decreased [46]. Figure 10 represents the contact angle images of the fabricated specimens.



Fig. 10. Contact Angle Images for (a) Pure PVA 2% (b) Pure PVA 5% (c) Pure PVA 10% (d) PVA 2%/BG 2% (e) PVA 5%/BG 2% (f) PVA 10%/BG 2%.

The addition of BG demonstrates an insignificant impact in contact angles due to BG incorporation. This is attributable to a low BG concentration of 2% and uniform embedding of BG within the PVA matrix. The fabricated specimens exhibit contact angles of less than 90° , proving that they are hydrophilic. The observed hydrophilic behavior of the fabricated specimens is quite similar as mentioned in the previous study [57]. It is evident from figure 11 that Pure PVA specimens with 2% PVA concentration depict the most hydrophilic behavior with a contact angle value of $43.4^\circ \pm 9.6^\circ$ and 10% (w/v) Pure PVA specimens represent the least hydrophilic behavior with the contact angle value of $86.7^\circ \pm 6.2^\circ$. It can be noticeable from the results that with the addition of BG the

contact angle is increased denoting that the wettability of the specimens is decreased and surface roughness is also increased. This indicates that the BG particles are slightly more hydrophobic than PVA molecules.

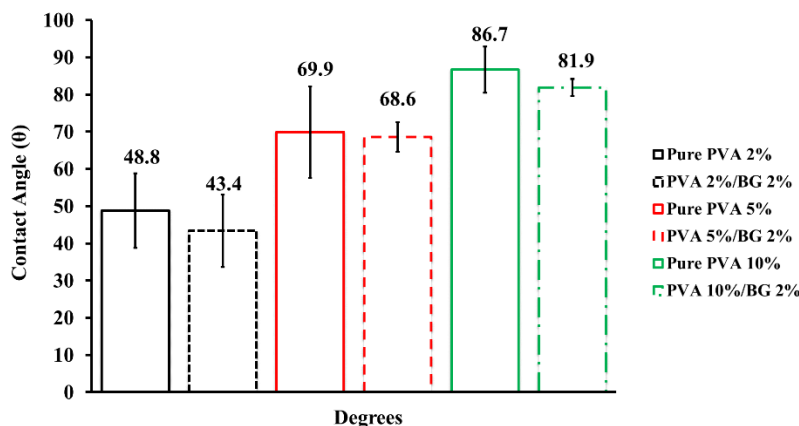


Fig. 11. Contact Angle Results of Pure PVA 2%, PVA 2%/BG 2%, Pure PVA 5%, PVA 5%/BG 2%, Pure PVA 10%, and PVA 10%/BG 2%.

3.8. Gel fraction

Gel Fraction test was performed to analyze the degree of crosslinking formed within a hydrogel structure. The greater the crosslinking, the higher the gel fraction is present in the hydrogel [56]. The swelling ability of the hydrogels is inversely proportional to the gel fraction value as with the increase in PVA concentration, there is more crosslinking and the space and volume for water uptake is reduced [38]. The results show that the gel fraction of the specimens do not differ significantly ($p > 0.05$) with the addition of Bio-Glass. However, as the concentration of PVA increases, a significant difference ($p < 0.05$) is noticeable among the specimens. Results indicated in figure 12 represent that with the addition of Bio-Glass, there is an increase in gel fraction. Furthermore, it can also be observed that with the increase in PVA concentration, there is also an increase in gel content which is similar to the results represented in [58].

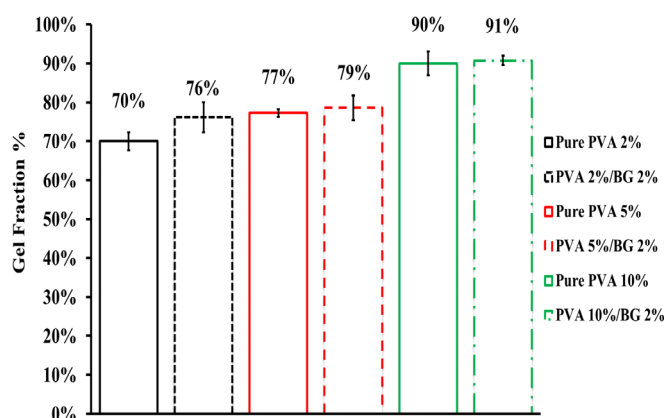


Fig. 12. Gel Fraction % of Pure PVA 2%, PVA 2%/BG 2%, Pure PVA 5%, PVA 5%/BG 2%, Pure PVA 10%, and PVA 10%/BG 2%.

It is evident from the results that the maximum gel fraction was observed in 10% (w/v) PVA/BG specimens that is $91\% \pm 0.0122\%$ and the least gel content was observed by 2% (w/v) Pure PVA specimens that is $70\% \pm 2.31\%$.

3.9. Water vapor transmission rate

Hydrogels used for wound healing applications must have an optimum water vapor transmission rate (WVTR), which means they must be capable of reducing the body's liquid loss by controlling the fluid absorption and transmission from the wound surface while keeping the humidity high [59]. The WVTR of the top surface of the wound dressings determines the moist environment of the wound which is crucial for wound healing. High WVTR represents rapid water loss and results in dehydration which in turn slows down the wound healing process whereas low WVTR results in exudate retention and promotes bacterial growth [60]. The WVTR value for normal skin was reported around $200 \text{ g/m}^2 \cdot \text{day}$, for a first-degree burn it was around $300 \text{ g/m}^2 \cdot \text{day}$ and, for granulating wounds it was reported around $500 \text{ g/m}^2 \cdot \text{day}$ [56]. The WVTR for wound dressing materials should be higher than the normal skin to provide an optimum environment for wound healing [61]. Therefore, the WVTR value for an ideal wound dressing should be between $2000 - 2500 \text{ g/m}^2 \cdot \text{day}$ [60]. However, the WVTR capability of the wound dressing needs to be higher, depending on the wound type. The ideal WVTR value for first-degree burns should be around $3000 \text{ g/m}^2 \cdot \text{day}$ whereas wound dressing for severe burns should be around $5000 \text{ g/m}^2 \cdot \text{day}$ [62]. WVTR values for Pure PVA and PVA/BG specimens were in between 2200 to $5000 \text{ g/m}^2 \cdot \text{day}$. It can be observed from the results that the gel fraction of the specimens represents no significant difference ($p > 0.05$) with the addition of Bio-Glass whereas with the increase in PVA concentration, a significant difference ($p < 0.05$) is observed in between specimens. The WVTR value is decreased with the increase in PVA concentration and with the addition of Bio-Glass as depicted in figure 13. PVA 2% exhibits the high value of WVTR i.e. $4989.6 \text{ g/m}^2 \cdot \text{day} \pm 498.96 \text{ g/m}^2 \cdot \text{day}$ whereas the least value of WVTR is observed in PVA (10%)/BG (2%) specimens i.e. $2245.3 \text{ g/m}^2 \cdot \text{day} \pm 249.48 \text{ g/m}^2 \cdot \text{day}$

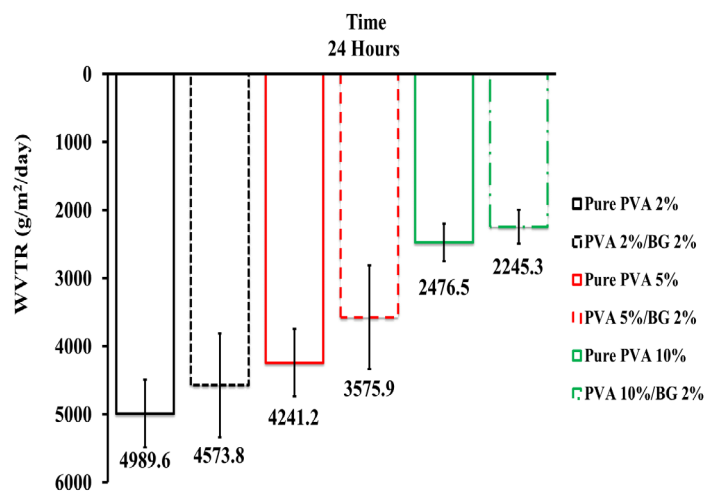


Fig. 13. WVTR of Pure PVA 2%, PVA 2%/BG 2%, Pure PVA 5%, PVA 5%/BG 2%, Pure PVA 10%, and PVA 10%/BG 2% over 24 hours.

4. Conclusion

This research focuses on the fabrication of a new biomaterial composite by incorporating polyvinyl alcohol and bio-glass. Both materials are proclaimed to be biocompatible, and biodegradable hence they are a choice for wound healing applications. promote wound healing. The composite is fabricated using the freeze-thaw method in three different concentrations of PVA i.e., 2%, 5%, and 10% whereas the concentration of BG is kept constant i.e. 2% The fabricated composite demonstrates optimal pH stability, degradation, swelling, gel fraction, wettability, hygroscopicity, WVTR, and tensile capabilities to be used for tissue engineering applications. Results indicated that with the increase in PVA concentration, there is a significant difference ($p < 0.05$) is observed in

between specimens. Furthermore, in degradation, swelling, and pH analysis, the addition of BG also depicts a significant difference ($p < 0.05$) in specimens of 2% concentration. The SEM analysis showed that the BG particles are well incorporated at 2% and 5% concentrations of PVA, as the particles amalgamate with the PVA whereas, at 10% concentration of pure PVA, the BG particles are visible on the surface. It was interesting to observe that a specimen with 2% pure PVA concentration exhibits excellent swelling capabilities, hydrophilicity, and, hygroscopicity.

Moreover, the specimens with 10% pure PVA concentration exhibit higher tensile strength and gel fraction, and their degradation rate is also faster than 2% and 5% pure PVA specimens. It is quite evident from the results that with the addition of BG, tensile strength, degradation rate, pH sensitivity, hydrophilicity, gel fraction, and swelling capability is increased, and WVTR is decreased. Results also indicate that 2% pure PVA specimens exhibit rapid swelling and degradation behavior whereas the PVA/BG specimens exhibit a slower degradation rate as compared to pure specimens at pH values 2.25, 4.6, 6.15, and 7.4. To our surprise, the addition of BG did not demonstrate any profound effect on hygroscopicity as expected. It is concluded that the fabricated material exhibits sufficient physical, chemical, and mechanical properties, and can be utilized for wound healing applications. Furthermore, antimicrobial and animal studies must be conducted in the future to assess its biocompatibility and biological performance. The new material will open new doors and widen the research perspective regarding the utilization of BG for soft-tissue regeneration.

Acknowledgments

The authors would like to acknowledge Dr. Aqeel, Dr. Ghazala, Mr. Tehseen, Mr. Waqas, and Engr. Shalani Nathaniel for their guidance and support throughout the research study. The authors would like to thank Salim Habib University, Biosciences, and Pharmacy department for providing the necessary lab resources.

References

- [1] J. Zhou et al., Mater. Sci. Eng. C, vol. 60, pp. 437-445, 2016; <https://doi.org/10.1016/j.msec.2015.11.068>
- [2] M. Bahadoran, A. Shamloo, and Y. D. Nokoorian, Sci. Rep., vol. 10, no. 1, pp. 7-9, 2020; <https://doi.org/10.1038/s41598-020-64480-9>
- [3] Y. Liang, B. Chen, M. Li, J. He, Z. Yin, and B. Guo, Biomacromolecules, vol. 21, no. 5, pp. 1841-1852, 2020; <https://doi.org/10.1021/acs.biomac.9b01732>
- [4] M. Sinha, J. Pharmacol. Ther. Res., vol. 02, no. 01, pp. 2-4, 2018, doi: 10.35841/pharmacology.2.1.1-3; <https://doi.org/10.35841/pharmacology.2.1.1-3>
- [5] R. F. Pereira, A. Mendes, and P. J. Bártolo, Chem. Eng. Trans., vol. 32, pp. 1009-1014, 2013.
- [6] N. H. Nicol, Dermatol. Nurs., vol. 17, no. 1, p. 62, 2005; https://doi.org/10.4324/9780203450505_chapter_1
- [7] G. Han and R. Ceilley, Adv. Ther., vol. 34, no. 3, pp. 599-610, 2017; <https://doi.org/10.1007/s12325-017-0478-y>
- [8] M. R. El-Aassar et al., Int. J. Biol. Macromol., vol. 167, pp. 1552-1563, 2021; <https://doi.org/10.1016/j.ijbiomac.2020.11.109>
- [9] T. Velnar, T. Bailey, and V. Smrkolj, J. Int. Med. Res., vol. 37, no. 5, pp. 1528-1542, 2009; <https://doi.org/10.1177/147323000903700531>
- [10] M. R. El-Aassar, O. M. Ibrahim, M. M. G. Fouda, N. G. El-Beheri, and M. M. Agwa, Carbohydr. Polym., vol. 238, no. March, p. 116175, 2020; <https://doi.org/10.1016/j.carbpol.2020.116175>
- [11] S. Dhivya, V. V. Padma, and E. Santhini, Biomed., vol. 5, no. 4, pp. 24-28, 2015; <https://doi.org/10.7603/s40681-015-0022-9>

- [12] Y. Liang, J. He, and B. Guo, *ACS Nano*, vol. 15, no. 8, pp. 12687-12722, 2021; <https://doi.org/10.1021/acsnano.1c04206>
- [13] E. Rezvani Ghomi, S. Khalili, S. Nouri Khorasani, R. Esmaeely Neisiany, and S. Ramakrishna, *J. Appl. Polym. Sci.*, vol. 136, no. 27, pp. 1-12, 2019; <https://doi.org/10.1002/app.47738>
- [14] J. Lei, L. Sun, P. Li, C. Zhu, and Z. Lin, *Heal. Sci J*, vol. 13, no. 4, p. 662, 2019.
- [15] S. N. F. M. Noor, N. S. M. Zain, P. Y. Wei, N. S. Azizan, and H. Mohamad, *AIP Conf. Proc.*, vol. 1791, no. December 2016, 2016; <https://doi.org/10.1063/1.4968872>
- [16] J. Elfar, R. M. G. Menorca, J. D. Reed, and S. Stanbury, "Composite bone models in orthopaedic surgery research and education," *J. Am. Acad. Orthop. Surg.*, vol. 22, no. 2, pp. 111–120, 2014, doi: 10.5435/JAAOS-22-02-111.
- [17] N. Al-harbi et al., *Silica-Based Bioactive Glasses and Their Applications in Hard Tissue Regeneration : A Review*, pp. 1-19, 2021; <https://doi.org/10.3390/ph14020075>
- [18] T. A. Van Vugt, J. A. P. Geurts, J. J. Arts, and N. C. Lindfors, *Biomaterials in treatment of orthopedic infections*. Elsevier Ltd., 2017; <https://doi.org/10.1016/B978-0-08-100205-6.00003-3>
- [19] J. Li, J. Chen, and R. Kirsner, *Clin. Dermatol.*, vol. 25, no. 1, pp. 9-18, 2007; <https://doi.org/10.1016/j.clindermatol.2006.09.007>
- [20] B. Guo, R. Dong, Y. Liang, and M. Li, *Nat. Rev. Chem.*, vol. 5, no. 11, pp. 773-791, 2021; <https://doi.org/10.1038/s41570-021-00323-z>
- [21] Y. Xu, J. Peng, X. Dong, Y. Xu, H. Li, and J. Chang, *Acta Biomater.*, vol. 55, pp. 249-261, 2017; <https://doi.org/10.1016/j.actbio.2017.03.056>
- [22] H. Li, Z. Wu, Y. L. Zhou, and J. Chang, *Bioglass for skin regeneration*. Elsevier Ltd, 2019; <https://doi.org/10.1016/B978-0-08-102546-8.00008-X>
- [23] R. Sergi, D. Bellucci, and V. Cannillo, *Materials (Basel)*, vol. 13, no. 23, pp. 1-38, 2020; <https://doi.org/10.3390/ma13235560>
- [24] S. Naseri, W. C. Lepry, and S. N. Nazhat, *J. Mater. Chem. B*, vol. 5, no. 31, pp. 6167-6174, 2017; <https://doi.org/10.1039/C7TB01221G>
- [25] S. Aruldass, V. Mathivanan, A. R. Mohamed, and C. T. Tye, *J. Environ. Chem. Eng.*, vol. 7, no. 5, 2019; <https://doi.org/10.1016/j.jece.2019.103238>
- [26] *Vinyl Additive Technology - 2021 - Bisht - Effect of functionalized silicon carbide nanoparticles as additive in.pdf*.
- [27] L. H. Gaabour and K. A. Hamam, *Dig. J. Nanomater. Biostructures*, vol. 15, no. 4, pp. 973-983, 2020; <https://doi.org/10.15251/DJNB.2020.154.973>
- [28] C. W. Schlickewei et al., *Int. J. Mol. Sci.*, vol. 20, no. 22, 2019; <https://doi.org/10.3390/ijms20225805>
- [29] A. Verma, *Appl. Sci. Eng. Prog.*, vol. 15, no. 2, pp. 1-13, 2022; <https://doi.org/10.14416/j.asep.2022.03.009>
- [30] W. Song, D. C. Markel, X. Jin, T. Shi, and W. Ren, *J. Biomed. Mater. Res. - Part A*, vol. 100 A, no. 11, pp. 3071-3079, 2012; <https://doi.org/10.1002/jbm.a.34240>
- [31] K. Kompany, E. H. Mirza, S. Hosseini, B. Pingguan-Murphy, and I. Djordjevic, "Polyoctanediol citrate-ZnO composite films: Preparation, characterization and release kinetics of nanoparticles from polymer matrix," *Mater. Lett.*, vol. 126, pp. 165–168, 2014, doi: 10.1016/j.matlet.2014.04.031.
- [32] A. Verma, N. Jain, K. Singh, V. K. Singh, S. M. Rangappa, and S. Siengchin, *Biodegrad. Polym. Blends Compos.*, pp. 309-326, Jan. 2022; <https://doi.org/10.1016/B978-0-12-823791-5.00010-7>
- [33] S. Sakai, M. Tsumura, M. Inoue, Y. Koga, K. Fukano, and M. Taya, *J. Mater. Chem. B*, vol. 1, no. 38, pp. 5067-5075, 2013; <https://doi.org/10.1039/c3tb20780c>
- [34] A. Priya, S. Nath, K. Biswas, and B. Basu, *J. Mater. Sci. Mater. Med.*, vol. 21, no. 6, pp. 1817-1828, 2010; <https://doi.org/10.1007/s10856-010-4053-1>
- [35] H. M. Mousa et al., *Eur. Polym. J.*, vol. 129, no. March, p. 109630, 2020; <https://doi.org/10.1016/j.eurpolymj.2020.109630>

- [36] F. H. ElBatal and G. T. El-Bassyouni, *Silicon*, vol. 3, no. 4, pp. 185-197, 2011; <https://doi.org/10.1007/s12633-011-9095-6>
- [37] S. M. K. Naqvi et al., *Mater. Express*, vol. 11, no. 1, pp. 107-115, 2021; <https://doi.org/10.1166/mex.2021.1895>
- [38] F. During et al., Investigation of Swelling Ratio and Textures Analysis of Acrylamide-Nanocellulose Corncobs Hydrogel Investigation of Swelling Ratio and Textures Analysis of Acrylamide-Nanocellulose Corncobs Hydrogel; <https://doi.org/10.1088/1742-6596/1805/1/012036>
- [39] M. Nandhakumar, R. Gosala, and B. Subramanian, *Biotechnol. Lett.*, no. 0123456789, 2022; <https://doi.org/10.1007/s10529-022-03303-5>
- [40] E. H. Mirza, W. M. A. Bin Wan Ibrahim, B. Pingguan-Murphy, and I. Djordjevic, "Polyoctanediol citrate-zinc oxide nano-composite multifunctional tissue engineering scaffolds with anti-bacterial properties," *Dig. J. Nanomater. Biostructures*, vol. 10, no. 2, pp. 415–428, 2015.
- [41] Y. J. No et al., *ACS Biomater. Sci. Eng.*, vol. 6, no. 4, pp. 1887-1898, 2020; <https://doi.org/10.1021/acsbiomaterials.9b01716>
- [42] M. F. Al Rez et al., "Tubular poly(ϵ -caprolactone)/chitosan nanofibrous scaffold prepared by electrospinning for vascular tissue engineering applications," *J. Biomater. Tissue Eng.*, vol. 7, no. 6, pp. 427–436, 2017, doi: 10.1166/jbt.2017.1593.
- [43] N. Goudar et al., *J. Polym. Environ.*, vol. 29, no. 9, pp. 2797-2812, 2021; <https://doi.org/10.1007/s10924-021-02070-0>
- [44] H. Xu et al., *Biomed. Mater.*, vol. 2, no. 2, pp. 62-66, 2007; <https://doi.org/10.1088/1748-6041/2/2/002>
- [45] H. Chopra, S. Bibi, S. Kumar, M. S. Khan, P. Kumar, and I. Singh, *Gels*, vol. 8, no. 2, 2022; <https://doi.org/10.3390/gels8020111>
- [46] S. Gupta and T. J. Webster, Evolution of PVA gels prepared without crosslinking agents as a cell adhesive surface Evolution of PVA gels prepared without crosslinking agents as a cell adhesive surface, no. June, 2011; <https://doi.org/10.1007/s10856-011-4343-2>
- [47] N. Golafshan, R. Rezasani, M. T. Esfahani, M. Kharaziha, and S. N. Khorasani, Nanohybrid Hydrogels of Laponite : PVA-Alginate as a potential wound healing material. Elsevier Ltd., 2017; <https://doi.org/10.1016/j.carbpol.2017.08.070>
- [48] E. E. Doğan, P. Tokcan, M. E. Diken, B. Yilmaz, B. K. Kizilduman, and P. Sabaz, *Adv. Mater. Sci.*, vol. 19, no. 3, pp. 32-45, 2019; <https://doi.org/10.2478/adms-2019-0015>
- [49] X. Hu et al., *Int. J. Clin. Exp. Med.*, vol. 9, no. 2, pp. 708-716, 2016.
- [50] M. M. F. bin Mohamed and R. Mohamed, *Adv. Mater. Res.*, vol. 1113, pp. 122-126, 2015; <https://doi.org/10.4028/www.scientific.net/AMR.1113.122>
- [51] K. Kudo, J. Ishida, G. Syuu, Y. Sekine, and T. Ikeda-Fukazawa, *J. Chem. Phys.*, vol. 140, no. 4, 2014; <https://doi.org/10.1063/1.4862996>
- [52] S. Hocine, D. Ghemati, and D. Aliouche, *Polym. Bull.*, no. 0123456789, 2023; <https://doi.org/10.1007/s00289-022-04664-7>
- [53] H. Haidari, Z. Kopecki, A. T. Sutton, S. Garg, A. J. Cowin, and K. Vasilev, *Antibiotics*, vol. 10, no. 1, pp. 1-15, 2021; <https://doi.org/10.3390/antibiotics10010049>
- [54] A. Hendi et al., *Int. J. Nanomedicine*, vol. 15, pp. 3887-3901, 2020; <https://doi.org/10.2147/IJN.S245743>
- [55] Y. Tang, L. Pang, and D. Wang, *J. Non. Cryst. Solids*, vol. 476, no. July, pp. 25-29, 2017; <https://doi.org/10.1016/j.jnoncrysol.2017.07.017>
- [56] M. T. Khorasani, A. Joorabloo, A. Moghaddam, H. Shamsi, and Z. MansooriMoghadam, *Int. J. Biol. Macromol.*, vol. 114, no. 2017, pp. 1203-1215, 2018; <https://doi.org/10.1016/j.ijbiomac.2018.04.010>
- [57] E. A. El-Hefian, M. M. Nasef, and A. H. Yahaya, *E-Journal Chem.*, vol. 8, no. SUPPL. 1, pp. 91-96, 2011; <https://doi.org/10.1155/2011/543587>

- [58] E. A. Kamoun, X. Chen, M. S. Mohy, and E. S. Kenawy, Arab. J. Chem., vol. 8, no. 1, pp. 1-14, 2015; <https://doi.org/10.1016/j.arabjc.2014.07.005>
- [59] M. Kokabi and Z. M. Hassan, POLYMER PVA - clay nanocomposite hydrogels for wound dressing, vol. 43, pp. 773-781, 2007; <https://doi.org/10.1016/j.eurpolymj.2006.11.030>
- [60] P. I. Morgado, A. Aguiar-ricardo, and I. J. Correia, J. Memb. Sci., 2015; <https://doi.org/10.1016/j.memsci.2015.04.064>
- [61] Z. Ujang, A. Hazri, A. Rashid, S. K. Suboh, and A. S. Halim, Physical properties and biocompatibility of oligochitosan membrane film as wound dressing, vol. 12, no. 3, pp. 155-162, 2014; <https://doi.org/10.5301/jabfm.5000190>
- [62] M. M. Delavari, Applied Sciences Preparing and Characterizing Novel Biodegradable Starch / PVA-Based Films with Nano-Sized Zinc-Oxide Particles for Wound-Dressing Applications, 2022; <https://doi.org/10.3390/app12084001>